The Relation of Radar to Cloud Area–Time Integrals and Implications for Rain Measurements from Space

DAVID ATLAS* AND THOMAS L. BELL

Laboratory for Atmospheres, NASA Goddard Space Flight Center, Greenbelt, Maryland

(Manuscript received 21 May 1991, in final form 10 January 1992)

ABSTRACT

In this work we determine the relationships between satellite-based and radar-measured area–time integrals (ATI) for convective storms and show how both depend upon the climatological conditional mean rain rate R_c and the ratio of the measured cloud (or radar echo) area to the actual rain area of the storms. Arkin's GOES precipitation index (GPI) = GF_cT (mm) where F_c is the fraction of a 2.5° box in GATE [GARP (Global Atmospheric Research Program) Atlantic Tropical Experiment] having clouds with infrared (IR) brightness temperatures less than 235 K, $G = 3$ mm h^{-1}, and T is cloud duration. However, we show that G is the ratio of R_c to $\langle A_c\rangle/\langle A_r\rangle$ where A_c and A_r denote cloud and rain area, respectively. We have demonstrated that Arkin's GPI reaches a stable asymptotic value for boxes of 2.5° in size because they include a sufficient number of storm cells to ensure that 1) the sample R_c, and thus the probability density function (PDF) of R, are representative of those in the climatological population; and 2) the ratio of the averages $\langle A_c\rangle/\langle A_r\rangle$ is similarly representative of the typical storm structure for the climatic regime. As the space–time sampling domain decreases, the correlation of GPI with cloud fraction decreases because these conditions are not met. Also, as the spatial sampling domain decreases, G decreases and the ratio $\langle A_c\rangle/\langle A_r\rangle$ increases because the smaller areas tend to have a larger fraction of rain-free cloud. Since $\langle A_c\rangle/\langle A_r\rangle$ must vary with storm type and climatic regime, the asymptotic (large area) GPI developed for GATE is unlikely to be valid for other regions. Smith et al. have also found a satellite cloud ATI for individual convective storms in North Dakota using a threshold IR brightness temperature of 250 K. In this case, we find that the ratio of the cloud to radar ATIs increases with the total volumetric rainfall, presumably because the more intense storms are associated with stronger updrafts and upper-level divergence, thus causing the cloud areas to exceed the rain areas by progressively larger amounts. Nevertheless, if the relationship between cloud and radar ATI is a stable one for a sufficient sample domain in each climatic regime, as is to be expected, then the cloud ATI becomes as powerful an estimator of convective rain as is the radar ATI (Rosenfeld et al. and others). One of its most valuable applications would be in conjunction with a satellite radar and/or radiometer as proposed for the Tropical Rainfall Measuring Mission (TRMM). TRMM could then serve as a global calibrating device to eliminate systematic biases. The increased sampling rate with the geosynchronous ATI would greatly improve the accuracy of the rainfall estimates, resulting in rms errors of 15%–20% of the mean in 2.5° boxes and 12 h, as compared with the 10% error for monthly averages over 5° boxes anticipated for TRMM. Such estimates would be useful for regional- and global-scale monitoring and forecasting.

1. Introduction

In this paper we shall show that 1) the GOES precipitation index (GPI) of Arkin (1986) for convective storms, an area–time integral (ATI) for satellite cloud areas, is related to the ATI for radar-observed rain areas (Doneaud et al. 1984; Rosenfeld et al. 1990) as explained by Atlas et al. (1990a); 2) the quality of GPI-based rainfall estimates depends upon how well the cloud area is related to the rain area, as suggested by Lovejoy and Austin (1979), and the size of the sampling domain; and 3) the use of a GOES cloud ATI in conjunction with the radar ATI from a satellite such as the Tropical Rainfall Measuring Mission (TRMM—Simpson et al. 1988) will improve the accuracy of rainfall estimates and permit them to be made in much smaller space–time domains than the 1-month and 5° boxes anticipated for TRMM.

2. The basis of the ATI method

Atlas et al. (1990a) have shown that the volumetric rain flux from a storm cluster is given by

$$V/T = S_t\overline{A}_t, \tag{2.1}$$

where the overbar indicates time averaging. The flux may also be expressed by

$$V/T = R_c\overline{A}_r, \tag{2.2}$$

where V is the lifetime volumetric rainfall, T is the

* Distinguished Visiting Scientist.

Corresponding author address: Dr. Thomas L. Bell, NASA/Goddard Space Flight Center, Code 913, Greenbelt, MD 20771.

storm duration, A_r is the total rainy area, A_t is the area of rain within the threshold t (mm h^{-1}), and both areas are lifetime averages; R_c is the conditional climatological rain rate for the storms in the particular climatic regime, and S_t is the slope of the V–ATI relation, where

$$\text{ATI} = \overline{A}_t T.$$

Note that if the threshold rain rate of the observing instrument is significantly greater than zero, then one must account for the portion of the area that is omitted.

Using (2.1) and (2.2), we find

$$S_t = R_c(\overline{A}_t/\overline{A}_r)^{-1}, \tag{2.3}$$

$$S_t = \frac{\int_0^\infty RP(R)dR}{\int_t^\infty P(R)dR}. \tag{2.4}$$

Note that the denominator of (2.3) is simply the fraction of the average storm area contained within the threshold t (mm h^{-1}) and this is represented by the denominator in (2.4) where $P(R)$ is the probability density function of R considered as a random variable. Of course, the numerator of (2.4) is R_c, the conditional climatological rain rate. While R_c is shown as a constant in (2.2) and (2.3), (2.4) shows that it is an estimator of the climatological average rate and approaches the "true" climatological rate only when the sample distribution of R approaches that of the population. By the same token, the average ratio $(\overline{A}_t/\overline{A}_r)$ is also an estimator that approaches the "true" value under similar conditions. This occurs only when the sample space–time domain is sufficiently large or the individual storms closely resemble one another (Atlas et al. 1990b).

If we divide (2.1) by the observing area A_o, then the left-hand side becomes the areawide instantaneous *unconditional* rain rate, which includes both rainy and nonrainy areas; on the right-hand side we obtain $F_t = \overline{A}_t/A_o$. Thus,

$$\langle R\rangle T = S_t F_t T. \tag{2.5}$$

Using radar rain data for various climatic regimes, Rosenfeld et al. (1990) have shown that S_t increases almost linearly with t and varies from one regime to another. Of course, when the threshold is zero and all the rain is included, then (2.3) shows that $S_{(t=0)} = R_c$. Atlas et al. (1990b) have found a value of 4.4 mm h^{-1} from the GATE [Global Atmospheric Research Program (GARP) Atlantic Tropical Experiment] shipboard siphon raingages. Chiu (1988) found the conditional climatological radar rain rate for 4-km × 4-km bins is 3.99 mm h^{-1}. Here we use R_c = 4.4 mm h^{-1}.

Based upon work done in GATE (Richards and Arkin 1981; hereafter referred to as RA), Arkin (1986) has proposed the *GOES precipitation index* (mm),

$$\text{GPI} = GF_cT \tag{2.6}$$

where G = 3 mm h^{-1}, F_c is the fractional coverage of a 2.5° × 2.5° box covered by clouds having an infrared (IR) equivalent blackbody temperature (T_{BB}) less than 235 K, and T is the cloud duration in hours. We see that Eqs. (2.5) and (2.6) are identical if we let $S_t \to G$ and $F_t \to F_c$. In short, the GPI is simply another form of the ATI applied to clouds. RA recognized the similarity of their findings to those of previous investigators (Lovejoy and Austin 1979), who found tight relationships between rainfall and radar echo areas.

3. Rain–cloud area relations for GATE

Using Eq. (2.3) and letting $G = S_t$ it is readily shown that

$$G = R_c[\langle A_c\rangle/\langle A_r\rangle]^{-1}, \tag{3.1}$$

where $\langle A_c\rangle$ is the average area of the clouds within T_{BB} over the sample space–time domain and $\langle A_r\rangle$ is the average area of the rain. Letting G = 3 for the 2.5° × 2.5° box and R_c = 4.4 mm h^{-1} as noted for GATE, we find $[\langle A_c\rangle/\langle A_r\rangle]$ = 4.4/3 = 1.47; that is, under these conditions the area of the clouds within T_{BB} = 235 K is about 1.5 times the rain area. Moreover, since R_c is constant for each climatic regime and rain type, the ratio of cloud to rain area is inversely proportional to G.

In Fig. 1 we show the variation of G with averaging scale and equivalent blackbody cloud temperature for hourly averages in GATE phases I and III, as found by RA. Phase II differed significantly from the other phases (Hudlow 1979). The nature and implications of this difference will be discussed in section 6. We see that G increases with decreasing T_{BB} and with increasing averaging scale; that is, moving from the lower left of Fig. 1 to the upper right. The converse is true for

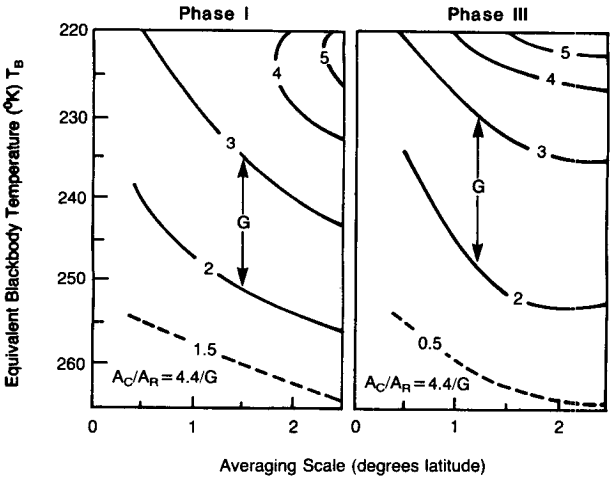

FIG. 1. The GPI index versus T_{BB} and averaging scale (degrees latitude) for 1-h averages in GATE phases I and III (after Richards and Arkin 1981).

$\langle A_c \rangle / \langle A_r \rangle$. It is evident that as T_{BB} decreases the area encompassed within the threshold decreases monotonically and it becomes a smaller and smaller fraction of the rainy area. The probable reason for the decrease of G and the increase of $\langle A_c \rangle / \langle A_r \rangle$ toward the smaller scales is discussed later. RA note that the correlation coefficient between the hourly estimated radar rainfall and the fractional cloud cover also decreases as we move to smaller scales, especially so as the scale falls below 1° or 100 km. They suggest that such low correlations are due to the influence of the life-cycle effects (i.e., variability of the R–F_c relation with lifetime of the storm) at such small scales. We shall provide an additional explanation later.

For a scale of 2.5°, Fig. 2 shows G versus T_{BB} and averaging interval for phases I and III. At this scale these parameters are essentially independent of the averaging time, and the ratio of cloud to rain area decreases monotonically with T_{BB} as before. However, because the correlations were strongest in the vicinity of 235 K, Arkin (1983) chose this temperature for his threshold and the associated $G = 3$ as the coefficient

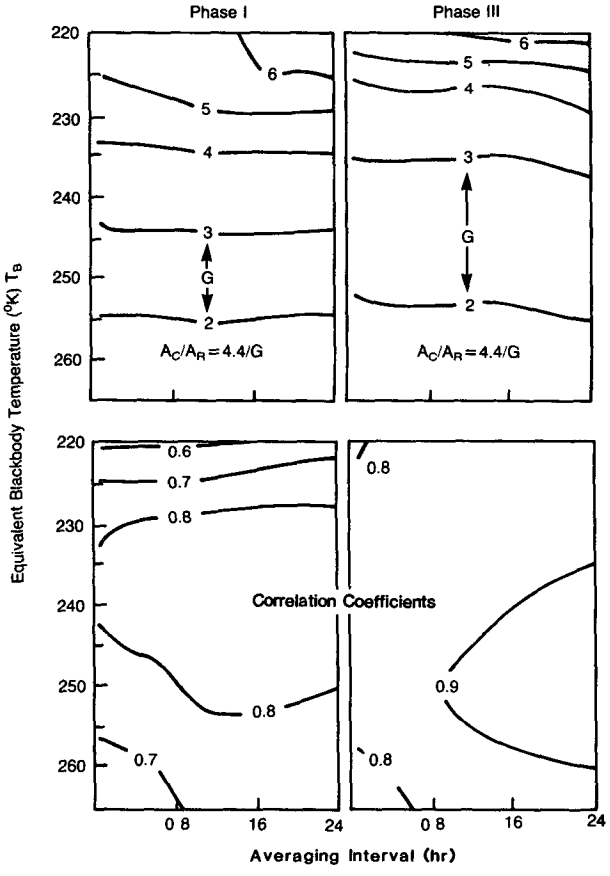

FIG. 2. The GPI index (upper panels) and regression correlation (lower panels) versus T_{BB} and averaging time for averaging boxes of 2.5° latitude in GATE phases I and III (after Richards and Arkin 1981).

of the GPI. Since $G = 3$ corresponds to $\langle A_c \rangle / \langle A_r \rangle = 1.47$ the 235-K threshold provides an average cloud area close to that of the rain area. We shall also see that the size of the averaging box is sufficient to provide a large enough sample of storm clouds such that the "average" cloud is typical of the local climatology, and the relation between the effective radar reflectivity Z_e and rain rate R settles down to that corresponding closely to a climatologically tuned relation (Atlas et al. 1990b). Returning to Fig. 1 we see that for hourly averages, one requires a larger spatial-averaging scale in order that G approach a constant value. This too was noted by RA.

In order to gain further insight into the reasons for such behavior we need the number of storm cells in the sampling domain. Houze and Cheng (1977) have shown that the probability distribution of storm-echo area in GATE is lognormal with μ = (mean $\ln A$) = 3.55, and σ = (standard deviation of $\ln A$) = 1.91. The average area is $\langle A \rangle = 215$ km^2. We now use Eqs. (2.3) and (2.5) to estimate S_t and F_t. The Houze and Cheng radar data had a minimum detectable reflectivity of 13.3 dBZ (at an rms range of 104 km; Hudlow et al. 1979), corresponding to a minimum R of 0.25 mm h^{-1} and an average ratio $\langle A_t \rangle / \langle A_r \rangle = 0.87$ (Atlas et al. 1990b); that is, 87% of the rainy area is detected. Using $R_c = 4.4$ mm h^{-1} and Eq. (2.3) we find $S_t = 5.1$ mm h^{-1}. Using the unconditional mean $\langle R \rangle = 0.5$ mm h^{-1}, $F_t = 0.1$; that is, 10% of the observing area must be covered by rain echoes in order to produce the reported mean rate. If the average storm area is only 215 km^2 then we require about 29, 10.5, and 1.2 storms to occupy the observing areas of 250, 150, and 50 km on a side, respectively, in order to produce the areawide mean rain rate. As the number of storms in the observing area increases, we may expect the sample rainfall statistics to approach that of the population, thereby better approximating the "true" values of R_c, $\langle R \rangle$, and S_t, provided that the storms are in various stages of their development. At the same time, we may use the Z–R relation for that climatic regime with greater confidence. Finally, it is also more likely that the ratio of the cloud area to rain area approaches the ratio typical of storms in that regime so that the coefficient G will have attained its asymptotic value for a large observing area.

These are the reasons that RA find that the correlation coefficients between the fractional cloud coverage F_c and $\langle R \rangle$ exceed .8 for observing boxes in excess of 1.5° (~150 km) on a side and for periods in excess of about 6 h. For a box of 2.5° (~250 km) on a side, the correlations are slightly larger and exceed .8 even for averaging periods as short as an hour. Also, the correlation coefficients increase with averaging time; that is, to a first approximation the correlation depends upon the space–time domain. At the smallest scale (~50 km on a side) in the RA study, the correlations are low because only one storm is needed to give the

GATE $\langle R \rangle$ and this is unlikely to produce sample statistics close to those of the population.

The behavior discussed in the foregoing may be understood better by referring to the algorithm of Stout et al. (1979). They report that the volumetric rain rate from an individual storm is given by the relation

$$V = a_0 A + a_1 \frac{dA}{dt} \tag{3.2}$$

where $a_0 = 5.4 \times 10^{-7}$ m s^{-1} and $a_1 = 2.8 \times 10^{-3}$ m, at an IR brightness temperature of 250 K. This is 15 K warmer than the temperature threshold used by RA. Using the mean values of A and $|dA/dt|$, they find that the two terms have mean values of 3.3×10^3 and 1.9×10^3 m^3 s^{-1}, respectively. Referring to the prior discussion we note that when there are a multiplicity of storms being observed simultaneously, Eq. (3.2) may be written as

$$V = a_0 \sum_i A_i + a_1 \sum_i \left(\frac{dA}{dt}\right)_i. \tag{3.3}$$

Also, when the storms are not evolving in phase with one another, the sum of the area change terms tends toward zero. With enough storm cells within the observing area, whatever the contributions of the derivatives, the average tends to be stable and is embedded in the area term itself. This is the case with the 2.5° box of RA.

On the other hand, in a small box of 0.5° (~50 km) on a side, we would typically have only a single storm (in GATE); sometimes none and other times a couple. In that case, some of these small boxes will contain only cloud and little if any rain. In other words, on a regression plot, there will be many points on the $R = 0$ axis and a relatively small number near the correct R–F location. This has the effect of decreasing G as observed by RA in Fig. 1. This can be seen in the scatterplot of Fig. 3b of RA for a 0.5° box and $T_{BB} = 240$ K. Also, the same figure shows that there are a substantial number of occasions in which the entire 0.5° box is covered by cloud (i.e., $F = 1.0$) while estimated rain rates range from 0 to more than 8 mm h^{-1}. Again the R–F locations of these observations are displaced from their proper positions, thereby producing an erroneous slope of the regression relation. On the other hand, there are a surprising number of points at zero fractional cloud cover with rain rates up to about 2.5 mm h^{-1}. This is probably attributable to three factors: 1) clouds with tops warmer than 240 K do in fact rain; 2) wind shear can readily cause the generating cloud to appear in one box while the rain falls into another; and 3) the thin diverging cirrus and altostratus that actually occur aloft have low emissivity and appear as warmer clouds with no rain. The second and third of these factors will clearly have more impact upon the correlations found in smaller boxes than in the larger ones. The net result is that the correlation coefficients found by RA for the smaller boxes and shorter periods are small. This is in accord with the experience of many investigators who have attempted to correlate the rain from individual storms with nearly simultaneous collocated satellite cloud images. In short, the cloud observations in small areas are unrepresentative of the area rainfall unless one takes very long-term averages.

One must also be careful to distinguish the behavior of the cloud areas in the two studies because of the warmer threshold IR temperatures used by Stout et al. (1979) to develop Eq. (3.2). In Fig. 1 we see that an increase in the IR threshold temperature, corresponding to a decrease in storm height, also tends to decrease G and, via Eq. (3.1), to increase $\langle A_c \rangle / \langle A_r \rangle$.

In short, the most important difference that accounts for the higher correlation coefficients observed by RA in the larger boxes is that it requires a sufficiently large space–time domain to obtain 1) a representative probability density function (PDF) of R and the corresponding moments (Atlas et al. 1990b), and 2) a stable climatological sample of the ratio of the average cloud area to the average rain area. Both of these are necessary to obtain a stable value of G. Accordingly, the larger number of storms in the 2.5° box will tend to give a closer approximation to the true $\langle R \rangle$ than will the one or two storms in the 0.5° box.

4. Rain–cloud area relation for North Dakota

Smith et al. (1990) have found a V–ATI cloud relationship for North Dakota based upon radar and GOES satellite data gathered in the northern High Plains of the United States during the summer of 1981. The radar data were collected at Bowman in southwestern North Dakota as part of the North Dakota Cloud Modification Project (NDCMP). The radar rain volume for each storm cluster was computed in a manner identical to that used by Doneaud et al. (1984) using the relation $Z = 155R^{1.88}$. A *storm cluster* was described as a *small mesoscale area* in the manner of Austin and Houze (1972) with areas between 50 and 1000 km^2, durations from about 0.5 to 2.5 h, and containing a multiplicity of individual cells. Others have called these clusters *convective complexes* (Heimbach and Super 1980). In order to find an optimum IR temperature threshold, they correlated cloud ATI with radar volumetric rainfall as a function of temperature. The best temperature was found to be 250 K, some 15 K warmer than the optimum threshold found by Richards and Arkin (1981). The area enclosed within this temperature contour was multiplied by the centered time interval for each image and summed over the lifetime of the event to derive the satellite ATI. Storm durations ranged from 0.5 to 4 h and the satellite image frequency ranged from 4 to 5 per hour.

They were able to obtain a total of 17 storm clusters that were not contaminated by extraneous clouds. Contamination occurs when storms merge or the storm

is well developed and the cirrus tends to obscure the end of the event. The resulting log–log scattergram and regression line are shown in Fig. 3. The correlation coefficient is .93 and the slope is 0.698. The rms logarithmic error is 0.28 (i.e., about a factor of 1.9). The regression equation is

$$V = 13.75(AT_c)^{0.698}, \quad (4.1)$$

where the subscript c signifies cloud and the constant has dimensions of $(\text{mm h}^{-1})(\text{km}^2\text{ h})^{0.302}$. While cirrus contaminate the observations in the latter stages of a storm, we note that the convective–stratiform technique (CST) of Adler and Negri (1988) provides a means of distinguishing the convective regions from the cirrus by texture analysis. This is thought to be one of the reasons that their method of estimating rainfall from IR imagery results in the best estimates of all the approaches used to date; see section 5b.5.

We have superimposed the radar V–ATI curve of Doneaud et al. (1984) obtained during the same project in North Dakota by the dashed line in Fig. 3. The latter was based upon 583 clusters. Here the ATI was determined for a threshold of 25 dBZ or 1.5 mm h^{-1} (using the aforementioned Z–R relation). The corresponding regression relation is

$$V = 3.7(AT_r). \quad (4.2)$$

We see that at $V > 285$ km^2 mm the cloud ATI begins to exceed the radar ATI and the excess increases with V. This is physically reasonable since the cloud begins to expand rapidly once its top approaches the tropopause. One cannot trust the cloud curve below its intersection with the radar curve because this implies that the cloud area is less than the 25-dBZ rain area, a physically implausible condition. (Alternatively, it is possible that the one point below the intersection is due to rain from a rather warm cloud.) In any case, using (4.1) and (4.2), the ratio of the cloud to radar ATI is given by

$$(AT_c)/(AT_r) = 0.08656V^{0.433} \quad (V > 285 \text{ km}^2 \text{ mm}) \quad (4.3)$$

where the constant has dimensions of $(\text{km}^2\text{ mm})^{-0.433}$. Using (4.2) we find

$$(AT_c)/(AT_r) = 0.1525(AT_r)^{0.433} \quad [(AT_r) > 77 \text{ km}^2 \text{ h}] \quad (4.4)$$

where the constant has dimensions of $(\text{km}^2\text{ h})^{-0.433}$. We see that when $V = 10^4$ km^2 mm and $AT_r = 2.7 \times 10^3$ km^2 h the ratio of the cloud to the 25-dBZ radar areas is 4.67. With such a storm of 1-h duration and dimensions of 52 km on a side, one obtains a total rainfall of 3.7 mm. It is apparent from Fig. 3 that 1) the cloud ATI is a reasonable measure of the storm or cluster rain volume, and 2) once the radar ATI reaches a threshold of 77 km^2 h, the cloud ATI increases at a faster pace than the radar ATI. The reason for this is that the depth, height, and updraft strength all increase with the storm area (Dennis et al. 1975). Thus, the greater the storm area, the greater will be the divergence near the tropopause, and the larger will be the ratio of the cloud to rain area. This is not to imply that the diverging upper-level cloud does not precipitate, but that it produces stratiform rain in which the rain rate per unit area is less than that in the convective portions of the storm. However, in all of this we must be careful to distinguish between the behavior of the storms in North Dakota, which commonly occur in a region of strong upper-level winds, and those in the tropical Atlantic where this is not the case.

It is useful to compare the storm areas treated by Smith et al. (1990) to those of Richards and Arkin (1981). The maximum AT_c is about 10^5 km^2 h and maximum duration is 4 h; this corresponds to a maximum cloud area of about 2.5×10^4 km^2 and a dimension of about 120 km on a side. This is about half the 250-km scale at which RA found the GPI coefficient to be reasonably constant in GATE. More typical dimensions for 1-h storms are 30–40 km. We have already noted that the GATE coefficient decreases to values of about 0.5–1 at scales of about 50 km, indicating that the cloud area at such a scale overestimates the rainy area by a factor of about 9 to 4.5, respectively. In other words, the behavior of the cloud to rain area ratio for GATE is not very different from that found in North Dakota for the smaller scales and warmer IR thresholds.

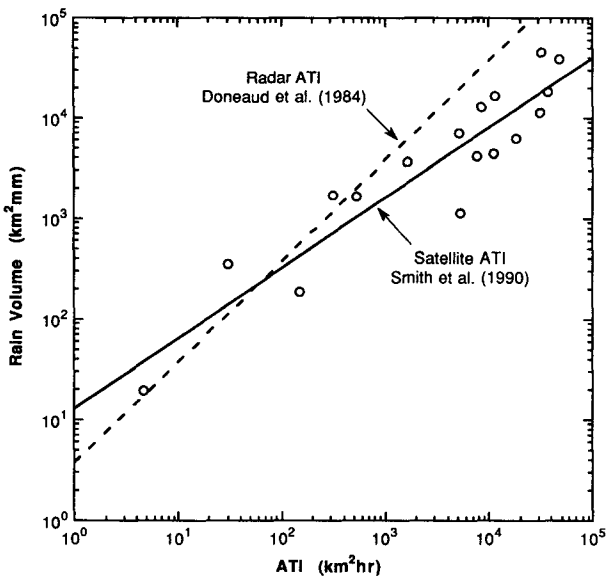

FIG. 3. Scatterplot of radar rain volume versus satellite ATI (T_{BB} = 250 K) for 17 rain clusters and regression line (solid) (after Smith et al. 1990), and original radar ATI relation of Doneaud et al. (1984) (dashed line) for North Dakota.

5. Combining TRMM and geosynchronous data

When averaged over a sufficient space–time domain, it is clear that 1) the cloud ATI is a useful measure of storm rain volume, and 2) it is also related in a reasonably well-defined manner to the radar ATI. If similar relationships can be found for other climatic regimes, then it has important implications for the measurement of convective rain from space. In particular, one of the key algorithms that has been proposed for use on the TRMM satellite is based upon the height–area rain threshold (HART) method of Rosenfeld et al. (1990). This is essentially an ATI method in which the areawide instantaneous rain rate is related to the fractional rainfall area above a specified rain-rate threshold as observed by a spaceborne radar; the addition of a measure of storm height improves the accuracy of the rain-rate estimate.

However, whether using HART or any other algorithm, the accuracy of the estimates is severely limited by the small number of storm samples that can be observed by a low-orbiting satellite during a single orbit. For this reason, the basic design of the TRMM proposes averaging measurements of rainfall over a domain of 500×500 km^2 and a period of a month (Simpson et al. 1988). In the course of a month the satellite revisits each area many times, thereby increasing the number of samples. Moreover, the orbit was designed to precess during the month in order to sample the rainfall during every clock hour and so compensate for possible biases due to diurnal variations of the rainfall. Based on GATE statistics, TRMM's averaging domain should provide an estimate of the mean rainfall accurate to 10% (Shin and North 1988; Bell et al. 1990).

Measurements of average rain rates over smaller space–time domains are clearly desirable. For example, for purposes of global weather prediction one would prefer to have rainfall observations on the scale of GCMs (e.g., 200 km on a side) and time periods of the order of 12 h. Using low-orbiting satellites like TRMM alone, however, the sampling errors would be too large. Our preceding discussion suggests that cloud observations from geosynchronous satellites can be used to fill in between the passes of the low-orbiting satellites and thus increase the number of samples, as well as observe the diurnal cycle. Instead of about 2 samples (or fewer) per day observed with the low orbiter, the synchronous satellite would make 48 observations per day at the present observing cycle of 2 per hour.

In the next two subsections we divide the mean-square error for geosynchronous data into sampling and measurement components and discuss the size of each. We show that sampling error is reduced to perhaps 5% and that retrievals might achieve accuracies of ~15%–20% for 12-h averages of rainfall on GCM scales.

a. Sampling error for geosynchronous observations

To establish notation, it will be useful to review briefly how mean-square error can be separated into sampling and measurement components. Let $R(t)$ (mm h^{-1}) be the instantaneous rain rate averaged over an area A at time t. The average rain rate during a period of length T (which we shall later take to be 12 h) is

$$\bar{R} = \frac{1}{T}\int_0^T R(t)dt. \tag{5.1}$$

The geosynchronous satellite estimate of $\bar{R}$ is inaccurate both because it is based on an average of noncontinuous observations made at intervals $\Delta t \approx 0.5$ h (sampling error) and because the measurements themselves are inaccurate (retrieval error). If we denote by $\hat{R}(t_i)$ the satellite estimate of area-averaged rain rate at observation time t_i, then the satellite estimate of $\bar{R}$ can be written

$$\hat{\bar{R}} = \frac{1}{N}\sum_{i=1}^{N}\hat{R}(t_i), \tag{5.2}$$

where the observation times t_i are all within the period T of interest.

We shall use the total mean-square error of the satellite estimates,

$$e_T^2 \equiv \langle(\hat{\bar{R}} - \bar{R})^2\rangle, \tag{5.3}$$

as a measure of the size of the error of a typical satellite estimate (5.2), where the brackets $\langle\ \rangle$ indicate an average over an ensemble of months with similar rainfall climatologies; that is, the "weather" over the area might vary among the different months in the ensemble, but the weather events during each month are consistent with the season and local "climate."

Let us also introduce the satellite estimate of (5.1) that would be obtained if the satellite could measure rain rates perfectly (i.e., measurements are exact but are made only at satellite observation times),

$$\bar{R}_S = \frac{1}{N}\sum_{i=1}^{N}R(t_i), \tag{5.4}$$

and write (5.3) as

$$e_T^2 \equiv \langle(\hat{\bar{R}} - \bar{R}_S + \bar{R}_S - \bar{R})^2\rangle,$$

which can be expanded as

$$e_T^2 = e_R^2 + e_S^2 + 2e_{RS}, \tag{5.5}$$

where

$$e_R^2 \equiv \langle(\hat{\bar{R}} - \bar{R}_S)^2\rangle = \left\langle\left\{\frac{1}{N}\sum_{i=1}^{N}[\hat{R}(t_i) - R(t_i)]\right\}^2\right\rangle \tag{5.6}$$

is the mean-square retrieval error,

$$e_S^2 \equiv \langle (\bar{R}_S - \bar{R})^2 \rangle = \left\langle \left[\frac{1}{N} \sum_{i=1}^{N} R(t_i) - \bar{R} \right]^2 \right\rangle \quad (5.7)$$

is the mean-square sampling error, and

$$e_{RS} \equiv \langle (\hat{\bar{R}} - \bar{R}_S)(\bar{R}_S - \bar{R}) \rangle \quad (5.8)$$

is their covariance. The covariance e_{RS} would be nonzero if unobserved rain is somehow correlated with retrieval error at the observation times. It seems reasonable to neglect this term, and we shall do so in the remainder of this discussion. The total mean-square error e_T^2 is thus the sum of sampling error and retrieval error.

Laughlin (1981) describes a method of estimating sampling error e_S^2 based on the assumption that the autocovariance of $R(t)$ has the form

$$\langle R'(t+\tau)R'(t) \rangle = \sigma_A^2 \exp(-|\tau|/\tau_A), \quad (5.9)$$

where

$$R'(t) = R(t) - \langle R(t) \rangle, \quad (5.10)$$

and σ_A^2 and τ_A are the variance and correlation time, respectively, of instantaneous area-averaged rain rate for the area A. For observations made at equally spaced intervals Δt, Laughlin (1981) obtained e_S^2 as a function of σ_A^2, τ_A, and T. His calculation is reviewed by Shin and North (1988). In the limit $\Delta t \ll \tau_A$, which is of interest to us, his result approaches

$$e_S^2 \approx \frac{\sigma_A^2}{T/\Delta t} \frac{\Delta t}{6\tau_A}. \quad (5.11)$$

[Sampling error is computed in this limit by North and Nakamoto (1989); their result, their Eq. (30), omits a factor of $\pi^2/6$.] The first term on the right-hand side of (5.11) is just the mean-square sampling error of an average of $T/\Delta t$ uncorrelated samples. The sampling error is reduced by the factor $\Delta t/6\tau_A$ because the unobserved rain in between the samples is correlated with the rain at the observed times. The reduction factor is linear in Δt because the correlation (5.9) falls off linearly with lag for small τ.

In order to proceed we require values for σ_A^2 and τ_A. We use values based on the rainfall statistics observed in GATE phase I, and shown in Table 1 for various areas with side L. These statistics are discussed in greater detail in Bell et al. (1990). The sampling error e_S, as a fraction of the mean rain rate $\bar{R} = 0.5$ mm h^{-1} for GATE phase I, is shown in Fig. 4 for various averaging periods T. Laughlin's exact result was used in these calculations, although approximation (5.11) is quite accurate for all but the smallest area.

TABLE 1. Variances and correlation times used in calculations of mean-square sampling errors for areas $A = L^2$.

L (km)	σ_A^2 (mm^2 h^{-2})	τ_A (h)
24	3.3	2.1
48	2.3	3.0
96	1.5	4.3
280	0.5	7.6

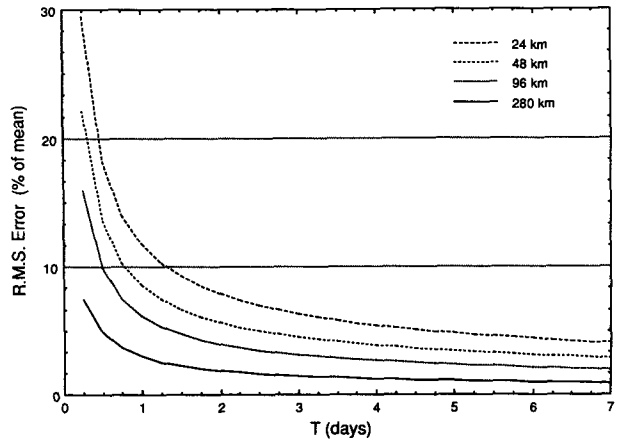

FIG. 4. Sampling error for space–time averages of rain rate, for averages of half-hourly samples taken over periods of length T, for four different size areas with dimensions L = 24, 48, 96, and 280 km. Error estimates are based on GATE statistics, with area mean rain rate of 0.5 mm h^{-1}.

It can be seen that the sampling error for 2.5° boxes (L = 280 km) and T = 12 h is less than 5%. Unlike the case of using TRMM data alone to estimate monthly averages, where sampling error dominates retrieval error (Bell et al. 1990; see also Wilheit 1987), the geosynchronous observations are frequent enough that inaccuracies in estimates of $\bar{R}$ are largely due to retrieval error. We turn next to a survey of typical retrieval errors encountered in retrieval of rainfall from visible and infrared data of the sort available from geosynchronous platforms.

b. *Geosynchronous retrieval errors*

Mean-square retrieval errors have been reported for estimates of average rainfall for various areas and periods, based on a number of algorithms using geosynchronous satellite data. We shall attempt to extrapolate these errors to values that might be encountered in estimating $\bar{R}$ for averaging period T = 12 h and A the area of a 2.5° box in the tropics. Some assumptions are needed to make these extrapolations, and we shall discuss them first before proceeding to individual retrieval methods and their errors.

Suppose a retrieval scheme makes an error $\epsilon(t)$ in retrieving the instantaneous area-averaged rain rate,

$$\epsilon(t) = \hat{R}(t) - R(t). \quad (5.12)$$

Lacking any information about the time correlation of $\epsilon(t)$, we shall assume that the errors behave like a first-order autoregressive process; that is, their statistics are

$$\langle \epsilon \rangle = 0, \tag{5.13}$$

$$\langle \epsilon^2 \rangle = \sigma_e^2, \tag{5.14}$$

$$\langle \epsilon(t+\tau)\epsilon(t) \rangle / \sigma_e^2 = e^{-|\tau|/\tau_e}. \tag{5.15}$$

Equation (5.13) implies that the retrieval scheme is unbiased in the long run. Comparison of geosynchronous estimates with the more direct measurements of satellites like TRMM will be essential in achieving this. Equation (5.15) implies that retrieval errors persist with a time constant (correlation time) τ_e. We neglect possible changes in the statistics with time, as, for example, with the time of day. This might be of concern when we extrapolate retrieval errors for which data are available only during daytime hours to nighttime periods.

Given these assumptions, the mean-square retrieval error e_R^2, Eq. (5.6), can be calculated for data sampled at equally spaced intervals Δt. Jones (1975) gives the result

$$e_R^2 = \frac{\sigma_e^2}{N}\left\{1 + 2\frac{\alpha}{(1-\alpha)^2}\left[(1-\alpha) - \frac{1}{N}(1-\alpha^N)\right]\right\} \tag{5.16}$$

for the variance of an average of N samples from a correlated time series, with correlation between successive samples

$$\alpha \equiv e^{-\Delta t/\tau_e}. \tag{5.17}$$

For N large, this is approximately

$$e_R^2 \approx \frac{\sigma_e^2}{N_{\text{eff}}}, \quad N_{\text{eff}} = \frac{N}{1 + 2\alpha/(1-\alpha)}. \tag{5.18}$$

That is, the variance of the average of the N correlated samples is the same as the average of N_{eff} independent samples. The greater the correlation α between samples, the fewer the effective number of samples N_{eff}. This concept is discussed further in Atlas (1964) and in greater detail in Lee (1960).

When the sampling interval is small compared with τ_e, Leith's (1973) expression for the variance of continuous averages over a time T can also be used:

$$e_R^2 \equiv \sigma_e^2 \frac{2G(T, \tau_e)}{T} \tag{5.19}$$

with

$$G(T, \tau_e) \equiv \tau_e\left[1 - \frac{\tau_e}{T}(1 - e^{-T/\tau_e})\right]. \tag{5.20}$$

Just as in (5.18), Eq. (5.19) can also be written as $\sigma_e^2/N_{\text{eff}}$, with $2G(T, \tau_e) \approx 2\tau_e$ the "time between effectively independent samples."

Most of the studies we shall discuss concentrated on estimating average rainfall for selected rainy periods, reporting the retrieval errors as fractional rms error

$$e_R/\langle \bar{R} \rangle. \tag{5.21}$$

In interpreting these errors, it should be noted that fractional rms error tends to be *less* when it is computed for selected rainy periods rather than for *arbitrary* periods, rainy or not. To see this, suppose that a retrieval method has rms error $e_{R,\text{rainy}}$ for rainy periods with mean rain rate $\bar{R}_{\text{rainy}}$, and suppose such rainy periods occur a fraction of the time f_{rainy}. Let us further suppose that the retrieval method can accurately distinguish rainy periods from nonrainy periods. Then the mean-square error for retrievals over an arbitrary period is $f_{\text{rainy}} e_{R,\text{rainy}}^2$, and the average rain rate is $f_{\text{rainy}}\bar{R}_{\text{rainy}}$, so the fractional error for arbitrary periods is

$$\frac{e_R}{\bar{R}} = \frac{1}{\sqrt{f_{\text{rainy}}}} \frac{e_{R,\text{rainy}}}{\bar{R}_{\text{rainy}}}. \tag{5.22}$$

It is larger than the fractional rms retrieval error $e_{R,\text{rainy}}/\bar{R}_{\text{rainy}}$ found for rainy periods alone! If, for instance, substantial rainy periods occurred only 25% of the time, the fractional error reported for arbitrary periods would be twice that for selected rainy periods. Unfortunately, it is not possible to estimate for realistic cases just how much the fractional error for selected periods underestimates that for arbitrary periods. We shall make some recommendations later about quantities that it would be very desirable to compute whenever retrieval errors are being reported.

We show in Fig. 5 the fractional rms errors [Eq. (5.21)] found by various authors, extrapolated by us to what their techniques might produce in estimating 12-h averages. The errors are shown as a function of

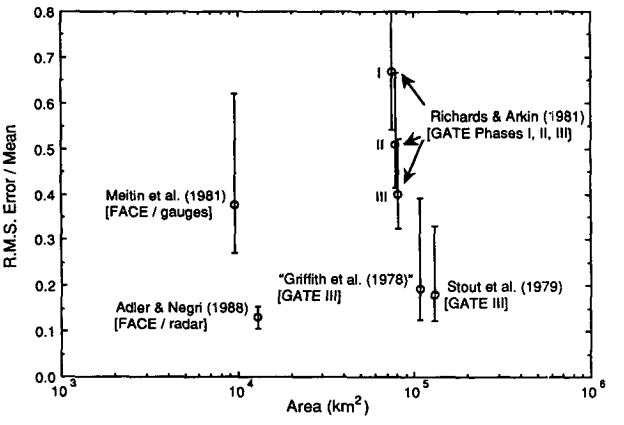

FIG. 5. Estimated fractional rms error of 12-h average rainfall versus averaging area for GATE and FACE from studies indicated. The 95% confidence intervals are based solely on number of samples used in studies.

the areas of each study. We shall describe next how each value plotted in the figure was obtained.

1) STOUT ET AL. (1979)

This study and the next two to be described used the GATE rainfall data to evaluate the accuracies of their methods. Stout et al. (1979) used instantaneous cloud area [defined as area with $T_{BB} \leq 250$ K for images from the Geostationary Meteorological Satellite (*SMS-1*)] and rate of change of cloud area as linear predictors of volumetric rain rate within the GATE phase III area (a circle of diameter 408 km). They report fractional errors 0.32 for 1-h averages and 0.23 for 6-h averages. If we assume that the rms error falls with averaging time T as in Eq. (5.16), we can explain this decrease with an error correlation time $\tau_e \approx 1.8$ h. Using Eq. (5.16) to extrapolate the error to $T = 12$ h, we obtain a fractional rms error of 0.18. (Note that this is quite close to $0.23/\sqrt{2}$; that is, errors in two successive 6-h periods are nearly independent.)

Because the rms error for 6-h averages was obtained by Stout et al. (1979) from a sample of about 10, we can compute confidence limits for the error if we assume the mean-square error is distributed like a chi-squared variable χ^2_ν with $\nu = (10 - 1) = 9$ degrees of freedom. Denote by $x_\nu(p)$ the value of χ^2_ν/ν such that

$$\Pr[\chi^2_\nu/\nu < x_\nu(p)] = p, \tag{5.23}$$

which can be looked up in standard statistical tables (Beyer 1981, for example); then the 95% confidence limits for the rms error are given by

$$\frac{\hat{\sigma}_R}{[x_\nu(0.975)]^{1/2}} < \sigma_R < \frac{\hat{\sigma}_R}{[x_\nu(0.025)]^{1/2}}, \tag{5.24}$$

where $\hat{\sigma}_R$ is the sample estimate from the study based on $\nu + 1$ samples. (See Jenkins and Watts 1968, p. 81, for example.) Our confidence limits are thus based on the assumptions that the cases studied are "representative" of the population of cases for which the retrieval method might be used, and also that the individual errors are roughly normally distributed. We have already argued that the fractional rms errors computed only from rainy periods underestimate the error for arbitrary periods. The error bars shown in Fig. 5 are based on these assumptions, and should probably be viewed as underestimates of the true confidence limits.

2) GRIFFITH ET AL. (1978)

Stout et al. (1979) also applied the Griffith et al. (1978) technique to the GATE data. The Griffith et al. (1978) technique (which we shall refer to as the NHEML technique) uses cloud-area history to estimate rainfall, associating different rain rates with different points in cloudiness evolution. Cloud area is delineated by $T_{BB} \leq 253$ K. The method was tuned using Florida precipitation data. Stout et al. (1979) report that, for an area equal to the overlap of the 408-km diameter GATE area and a 3° box, for eight 6-h periods, the correlation of the NHEML estimates with radar estimated rainfall was 0.85, whereas the correlation of Stout et al.'s estimates was 0.87. Assuming the same $\langle \bar{R} \rangle$ and error correlation time as in Stout et al.'s study, we would estimate the fractional rms error for the NHEML technique for 12-h averages to be larger by the factor $(1 - 0.85^2)^{1/2}/(1 - 0.87^2)^{1/2}$. Therefore, we estimate the fractional rms error for the Griffith et al. (1978) technique to be 0.19, with error bars based on (5.24) with $\nu = (8 - 1)$ degrees of freedom.

3) RICHARDS AND ARKIN (1981)

The authors applied their easily automated rainfall estimation procedure discussed earlier to 12-h periods in all three phases of GATE. They report means and σ_1 (the standard deviation of hourly averages over a 2.5° box) for each phase, and in their Fig. 6 give contours for the correlation (reproduced in our Fig. 2) of 12-h average rainfall against cloud area ($T_{BB} < 240$ K). We give these values in the first three columns of Table 2. It should be noted that the contour plots of correlation were widely spaced and so our values of the correlations may differ from the correct values by a few percent. To convert the regression correlation c_R into rms error e_R using

$$e_R^2 = \mathrm{var}(\bar{R})(1 - c_R^2), \tag{5.25}$$

we require the variance of 12-h average rainfall $\mathrm{var}(\bar{R})$—the "variance to be explained." We have estimated this from Leith's expression (5.19) for the variance of a time-averaged quantity, using $T = 12$ h and $\tau = 7.6$ h, the correlation time for GATE rainfall found in both phase I and phase II (Bell et al. 1990), and assumed to hold for phase III as well. We find

$$\mathrm{var}(\bar{R}) = 0.63\sigma_1^2,$$

based on which we have calculated the fractional rms error in the last column. The error bars shown in Fig. 5 are based on Eq. (5.24) with $\nu \approx 35$. (There are somewhat fewer 12-h periods in phase II.)

TABLE 2. Values used to estimate fractional rms error for retrievals of 12-h averaged rainfall $\bar{R}$, from Richards and Arkin (1981), using three phases of GATE data for verification. Means and standard deviations of hourly rainfall are shown in columns 2 and 3, correlation $\bar{R}$ with cloudiness index in column 4, the standard deviation of $\bar{R}$ in column 5, and the error in the last column.

GATE phase	$\langle \bar{R} \rangle$ (mm h^{-1})	σ_1 (mm h^{-1})	c_R	$\sqrt{\mathrm{var}(\bar{R})}$ (mm h^{-1})	$e_R/\bar{R}$ (%)
I	0.53	0.78	.82	0.62	67
II	0.41	0.52	.86	0.41	51
III	0.54	0.59	.89	0.47	40

4) MEITIN ET AL. (1981)

The two remaining studies used FACE (Florida Area Cumulus Experiment) data for training and verification of the methods. The results of Meitin et al. (1981) are summarized by Griffith (1987). They employed the Griffith et al. (1978) technique to estimate 6-h rainfall over the FACE area. We have extrapolated the rms error they found to that for 12-h averages by dividing the rms error by $\sqrt{2}$, that is, by assuming two consecutive 6-h errors are independent. It should be noted that this is the only study in Fig. 5 that used a dense array of raingages as "truth." The others used radar estimates. The confidence intervals are based on $\nu = (13 - 1)$, since rain estimates from 13 days were used to obtain the rms error.

5) ADLER AND NEGRI (1988)

The authors used their convective–stratiform technique to estimate rainfall for selected events over the FACE area. They found an rms error $\sigma_e = 0.78$ mm h^{-1} for half-hourly estimates for four days of data (6–8 h each day), with a mean of 1.98 mm h^{-1}, or a fractional rms error of 0.39. The standard deviation of the errors in the four daily estimates dropped to 0.35 mm h^{-1}, which Eq. (5.16) could explain if the error correlation time $\tau_e \approx 0.5$ h. This agrees qualitatively with the frequent sign change in the difference of CST-estimated rain depth and gauge-adjusted radar estimates shown in Figs. 4–7 of Adler and Negri (1988). We have extrapolated their rms error for half-hourly estimates to that of 12-h averages assuming $\tau_e = 0.5$ h, obtaining a fractional rms error of 0.13. Because of the short correlation time, we have used $\nu = (55 - 1)$ in obtaining the confidence limits for σ_R. Note that this case has required extrapolation to averaging times farthest from the averaging time for which rms error was calculated of any of the studies discussed here.

Richards and Arkin were the only authors to report fractional rms error for arbitrary periods instead of for selected periods. The fractional errors for all of the other studies are therefore lower by possibly a factor of 2 or more compared to what they would have computed had they not confined their investigations to selected rainy periods. Adler and Negri (1988), for example, found that RA's GPI threshold technique produced rms errors only 23% larger than their technique did when applied to the same selected cases. In making these comparisons, therefore, we cannot emphasize too much that some of the differences in the relative magnitudes of the errors found by RA and the other authors are due to the phenomenon we have described leading to Eq. (5.22).

Our extrapolations to periods different from those examined in the original retrieval studies required some statistical properties of the retrievals that are not customarily reported in such investigations. We would like to suggest that, where practicable, future retrieval studies include rms errors for their retrievals at the smallest time intervals for which retrievals are possible, as well as the time correlations of the errors and dependence on the area averaged over. It is clear from the discussion leading to Eq. (5.22) that fractional rms error can be a misleading measure of retrieval error. A better way of characterizing it is needed.

6. Discussion

For large areas, the rms error of a given technique probably decreases with area size as $1/\sqrt{A}$. Figure 5 therefore suggests that 12-h average rainfall over areas the size of GCM grid boxes can be estimated using geosynchronous data alone with an rms error that is 15%–20% of the mean. Rainfall estimates with this accuracy would be quite useful. It should be noted, however, that the most successful techniques in Fig. 5 were tuned to the local climatology. Although it appears that one would require neither the radar nor radiometers aboard TRMM as is now planned if one has access to geosynchronous cloud observations, it is important that they be used in combination in order to provide a means of calibrating the cloud ATI algorithm since the calibration is likely to change from one climatic regime to another. Convective storms, for example, which either reach the tropopause or occur in a strongly sheared environment, are likely to have a different ratio of cloud to radar ATI from those in other conditions.

As mentioned earlier, GATE phase II differed from the other two phases in several respects (see RA). First, phase II had systematically smaller hourly mean rain rates, standard deviations, and maxima, and the ratio of the mean rate in II to that in the other phases decreased sharply with the scale. At the 2.5° scale, the mean rate was less than that in the other two phases by about 25%; at the 0.5° scale it was about 75% less. The decrease with scale was due to the fact that the 0.5° scale (measured only around the center of the GATE array) fell entirely within a minimum in the phase II isohyetal pattern with a mean hourly rain rate of only 0.13 mm h^{-1}. This compares to values of about 0.5 mm h^{-1} in the other phases at all scales. Secondly, the very small rates at the smallest scale were also manifested by very low correlation coefficients between radar-estimated rainfall and fractional coverage, and unlike the other phases, the correlations did not increase with averaging time. It was only at the larger scales that the correlation coefficients approached those in phases I and III. RA note that "it appears that the relationship between rainfall and the fractional cloud coverage is better for periods and/or areas of significant rainfall. When precipitation is light, the one-parameter model may be incapable of achieving significant correlations."

However, the answer to the problem lies in the statement by RA that "the success of the simple linear

model [between areawide rainfall and fractional cloud cover, as in Eq. (2.6)] implies that most rain-producing cloud systems in GATE, when viewed over a large enough area, had an effective mean (conditional) rainfall rate that did not vary greatly from event to event." This is precisely the basis for good performance of the radar ATI as described by Atlas et al. (1990a) and as embodied in the set of equations (2.1) through (3.1). The 25% reduction in areal rain rate in phase II signifies that this phase was anomalous relative to the others either in the number of rain events or the conditional rain rate R_c per event. Hudlow and Patterson (1979) have shown that the fractional area covered by high clouds observed by satellite was also reduced by about this amount. This suggests that the smaller amount of rain during phase II was due to the frequency of rain rather than to R_c. Thus, the radar and cloud ATI relations should be affected only by the natural variability in $S(t)$ in Eq. (2.4) and G in Eq. (3.1).

On the other hand, if the climatic regime were to change in such a manner as to alter the nature of the rainstorms themselves, and thus to alter R_c, the use of the ATI method would be questionable. It would then be necessary to use an independent radar and/or radiometric measurement system on board the TRMM satellite, and also to employ a physically based algorithm such as those proposed by Meneghini et al. (1989) or Weinman et al. (1990). The latter are independent of the ATI method and should be capable of measuring the rain rates as well as the storm areas. In this way, the difference in the mean conditional rates would be detectable and the true rates would be measurable. Once TRMM has been calibrated against reliable ground-truth raingage networks, it then serves as a transfer standard with which to calibrate other instruments and algorithms such as the geosynchronous ATI method anywhere on the globe. It is in this sense that TRMM is a "flying raingage."

One of the arguments for the low inclination orbit of TRMM was the increased sampling the orbit made possible in the tropics. Because of the way in which the geosynchronous cloud observations support the radar and radiometer, the sampling characteristics of a TRMM-like satellite in a polar orbit might suffice. Such a satellite could then serve as a global calibrating device.

7. Conclusions

Although the area–time integral (ATI) has become an important basis for radar estimates of rain both from the surface and potentially from space, its use in space without a spaceborne radar depends upon the applicability of corresponding cloud ATIs either in the visible (VIS) or IR. Virtually all the algorithms developed to relate VIS and IR cloud areas to rainfall are in fact a form of cloud ATI when integrated over time and area. The GOES precipitation index (GPI) of Arkin is a well-established ATI that is in widespread use for estimating tropical convective rainfall. We have demonstrated that Arkin's GPI works in large part because the average cloud area $\langle A_c \rangle$ within a specified IR threshold is an estimator of the rain area $\langle A_r \rangle$. Its accuracy increases with the size of the sample space–time domain because the number of storm cells included in the sample increases and the average becomes more representative of the range of storm-cell structures and stages of development. The accuracy also increases with the sample size because the GPI coefficient is proportional to the conditional climatological rain rate R_c, the accuracy of which depends upon how well the sample probability density function (PDF) of R approaches that of the climatological population. Since both $\langle A_c \rangle / \langle A_r \rangle$ and R_c must vary with storm type and climatic regime, the GPI developed for GATE is unlikely to be valid for other regions. Thus, we need some means of calibrating the relation of the cloud ATI to the radar ATI and then to the areawide rainfall reaching the surface.

Smith et al. (1990) have also found a satellite cloud ATI for individual convective storms in North Dakota using a threshold IR brightness temperature of 250 K. In this case, we find that the ratio of the cloud to radar ATIs increases with the total volumetric rainfall, presumably because the more intense storms are associated with stronger updrafts and upper-level divergence, thus causing the cloud areas to exceed the rain areas by progressively larger amounts. Nevertheless, if the relationship between cloud and radar ATI is a stable one for a sufficient sample domain in each climatic regime, as is to be expected, then the cloud ATI becomes as powerful an estimator of convective rain as is the radar ATI (Rosenfeld et al. 1990 and others). We suggest that such cloud ATIs or GPIs can be found for the various regimes, thus making it a powerful estimator of convective rain.

One of its most valuable applications would be in conjunction with a satellite radar and/or radiometer as proposed for TRMM. TRMM could then serve as a global calibrating device to eliminate systematic biases. The increased sampling rate with the geosynchronous ATI would greatly improve the accuracy of the rainfall estimates, resulting in rms errors of 15%–20% of the mean in 2.5° boxes and 12 h as compared with the 10% error for monthly averages over 5° boxes anticipated for TRMM. Such estimates would be useful for regional- and global-scale monitoring and forecasting.

Acknowledgments. We appreciate the permission of Dr. Paul Smith of South Dakota Institute of Mining and Technology to utilize the data in Fig. 3. We are also indebted to Dr. David Short of NASA GSFC and Dr. Daniel Rosenfeld of Hebrew University, both of whom contributed stimulating ideas.

REFERENCES

Adler, R. F., and A. J. Negri, 1988: A satellite infrared technique to estimate tropical convective and stratiform precipitation. *J. Appl. Meteor.*, **27**, 30–51.

Arkin, P., 1986: Global large scale precipitation data sets for the WCRP, World Climate Research Program, WCP-111, WMO/TD-No.94, Geneva, Switzerland.

Atlas, D., 1964: Advances in radar meteorology. *Adv. Geophys.*, **10**, 317–478.

——, D. Rosenfeld, and D. A. Short, 1990a: The estimation of convective rainfall by area integrals. Part 1: The theoretical and empirical basis. *J. Geophys. Res.*, **95**, 2153–2160.

——, ——, and D. B. Wolff, 1990b: Climatologically tuned reflectivity–rain rate relations and links to area–time integrals. *J. Appl. Meteor.*, **29**, 1120–1135.

Austin, P. M., and R. A. Houze, Jr., 1972: Analysis of the structure of precipitation patterns in New England. *J. Appl. Meteor.*, **11**, 926–935.

Bell, T. L., A. Abdullah, R. L. Martin, and G. R. North, 1990: Sampling errors for satellite-derived tropical rainfall: Monte Carlo study using a space–time stochastic model. *J. Geophys. Res.*, **95D**, 2195–2205.

Beyer, W. H., 1981: *Handbook of Tables for Probability and Statistics*, 2nd Ed. CRC Press, 642 pp.

Chiu, L. S., 1988: Estimating areal rainfall from rain area. *Tropical Rainfall Measurements*, J. S. Theon and N. Fugono, Eds., A. Deepak Publishing, 361–367.

Dennis, A. S., A. Koscielski, D. E. Cain, J. H. Hirsch, and P. L. Smith, Jr., 1975: Analysis of radar observations of a randomized cloud seeding experiment. *J. Appl. Meteor.*, **14**, 897–908.

Doneaud, A. A., S. I. Niscov, D. L. Priegnitz, and P. L. Smith, 1984: The area–time integral as an indicator for convective rain volumes. *J. Climate Appl. Meteor.*, **23**, 555–561.

Griffith, C. G., 1987: Comparisons of gauge and satellite rain estimates for the central United States during August 1979. *J. Geophys. Res.*, **92D**, 9551–9566.

——, W. L. Woodley, P. G. Grube, D. W. Martin, J. Stout, and D. N. Sikdar, 1978: Rain estimation from geosynchronous satellite imagery—Visible and infrared studies. *Mon. Wea. Rev.*, **106**, 1153–1171.

Heimbach, J. A., Jr., and A. B. Super, 1980: Raingage network requirements from a simulated convective complex weather modification experiment. *J. Appl. Meteor.*, **19**, 1176–1183.

Houze, R. A., Jr., and C. P. Cheng, 1977: Radar characteristics of tropical convection observed during GATE: Mean properties and trends over the summer season. *Mon. Wea. Rev.*, **105**, 964–980.

Hudlow, M. D., 1979: Mean rainfall patterns for the three phases of GATE. *J. Appl. Meteor.*, **18**, 1656–1669.

——, and V. L. Patterson, 1979: *GATE Radar Rainfall Atlas*. Environmental Data and Information Service, NOAA, 155 pp.

Jenkins, G. M., and D. G. Watts, 1968: *Spectral Analysis and Its Applications*. Holden-Day, 525 pp.

Jones, R. H., 1975: Estimating the variance of time-averages. *J. Appl. Meteor.*, **14**, 159–163.

Laughlin, C. R., 1981: On the effect of temporal sampling on the observations of mean rainfall. *Precipitation Measurements from Space, Workshop Report*, D. Atlas and O. Thiele, Eds., NASA Goddard Space Flight Center, Greenbelt, MD, D59–D66.

Lee, Y. W., 1960: *Statistical Theory of Communication*. J. Wiley & Sons, 509 pp.

Leith, C. E., 1973: The standard error of time-average estimates of climatic means, *J. Appl. Meteor.*, **12**, 1066–1069.

Lovejoy, S., and G. L. Austin, 1979: The sources of error in rain amount estimating schemes from GOES visible and IR satellite data. *Mon. Wea. Rev.*, **107**, 1048–1054.

Meitin, J. G., C. G. Griffith, J. A. Augustine, and W. L. Woodley, 1981: A standard verification for rainfall estimation from remote platforms. *Precipitation Measurements from Space, Workshop Report*, D. Atlas and O. Thiele, Eds., NASA Goddard Space Flight Center, Greenbelt, MD, D94–D97.

Meneghini, R., K. Nakamura, C. W. Ulbrich, and D. Atlas, 1989: Experimental tests of methods for the measurement of rainfall rate using an airborne dual-wavelength radar. *J. Atmos. Oceanic Tech.*, **6**, 637–651.

North, G. R., and S. Nakamoto, 1989: Formalism for comparing rain estimation designs. *J. Atmos. Oceanic Technol.*, **6**, 985–992.

Richards, F., and P. Arkin, 1981: On the relationship between satellite-observed cloud cover and precipitation. *Mon. Wea. Rev.*, **109**, 1081–1093.

Rosenfeld, D., D. Atlas, and D. A. Short, 1990: The estimation of rainfall by area integrals. Part 2: The height–area rain threshold (HART) method. *J. Geophys. Res.*, **95**, 2161–2176.

Shin, K.-S., and G. R. North, 1988: Sampling error study for rainfall estimate by satellite using a stochastic model. *J. Appl. Meteor.*, **28**, 1218–1231.

Simpson, J., R. F. Adler, and G. R. North, 1988: A proposed Tropical Rainfall Measuring Mission (TRMM). *Bull. Amer. Meteor. Soc.*, **69**, 278–295.

Smith, P. L., Jr., L. R. Johnson, T. H. Vonder Haar, and D. Reinke, 1990: Radar and satellite area–time-integral techniques for estimating convective precipitation. Preprints, *Conf. on Operational Precipitation, Estimation, and Prediction*, Amer. Meteor. Soc., Anaheim, 32–35.

Stout, J., D. W. Martin, and D. N. Sikdar, 1979: Estimating GATE rainfall with geosynchronous satellite images. *Mon. Wea. Rev.*, **107**, 585–598.

Weinman, J. A., R. Meneghini, and K. Nakamura, 1990: Retrieval of precipitation profiles from airborne radar and passive radiometer measurements: Comparison with dual-frequency radar measurements. *J. Appl. Meteor.*, **29**, 981–993.

Wilheit, T. T., 1988: Error analysis for the Tropical Rainfall Measuring Mission (TRMM). *Tropical Rainfall Measurements*, J. S. Theon and N. Fugono, Eds., A. Deepak, 377–385.

Woodley, W. L., C. G. Griffith, J. S. Griffin, and S. C. Stromatt, 1980: The inference of GATE convective rainfall from *SMS-1* imagery. *J. Appl. Meteor.*, **19**, 388–408.